



## Optimizing Cr(VI) Reduction in Plastic Chromium Plating Wastewater: Particle Size, Irradiation, Titanium Dose

Angelica Santis <sup>1\*</sup> , Oscar Arbeláez <sup>2</sup>, Luz Angelica Cardenas <sup>1</sup>, Jaritza Castellanos <sup>1</sup>, Pablo Velasquez <sup>1</sup> 

<sup>1</sup> Ingenio Induspymes Research Group, Universidad Cooperativa de Colombia, Av. Caracas N° 37-63, Bogotá, Colombia.

<sup>2</sup> Termomec Research Group, Universidad Cooperativa de Colombia, Av. Colombia N° 41-26, Medellín, Colombia.

### Abstract

The preservation of the aquatic environment and water systems has been a fundamental objective that has led great scientists and researchers to seek new alternatives or techniques that allow the decontamination of water sources. The plastic chromium plating industries have been identified as important sources of contamination since their residues are characterized by having considerable amounts of hexavalent chromium Cr (VI), which alters the stability of water resources and can affect effluents on the surface and the subsoil. Given this problem, the need to improve the usual methods and techniques for wastewater treatment with more effective solutions, such as photocatalysis, which presents significant advantages over the inefficiency of traditional methods, is recognized. However, given the limited availability of research in the country that addresses the removal of hexavalent chromium from the wastewater of these industries, this work focuses on optimizing the process by varying conditions of variables such as particle size, catalyst dose, and irradiation time. The optimization of the photocatalysis process was evaluated using the Box-Behnken experimental design. The results show that contaminant removal occurred when the particle size was 0.177 mm. This particle size showed the highest photocatalytic activity, with 100% removal at 45 minutes. These findings represent a significant step towards solving the problem of contamination in this business sector by this pollutant and contribute to preserving our water resources.

### Keywords:

Photocatalysis;  
Box-Behnken Experimental Design;  
Particle Size;  
Catalyst;  
Hexavalent Chromium Cr (VI).

### Article History:

Received:	04	October	2023
Revised:	16	January	2024
Accepted:	21	January	2024
Published:	01	February	2024

## 1- Introduction

The tanning, electroplating, dyeing, pigment, and metallurgical industries, among others, use chromium (Cr) in their processes [1]. Effluents from these industries generate wastewater containing Cr (VI). This agent is not only highly polluting for the environment but also a mutagenic and carcinogenic cytotoxic agent, which is associated with a wide range of clinical effects and health risks, such as liver damage, lung carcinoma, ulcerations, and tract irritation gastrointestinal, and kidney damage when consumed above the allowed limit [2]. The maximum permitted limits of Cr (VI) in drinking water and its discharge into continental waters are 0.05 mg L<sup>-1</sup> and 0.1 mg L<sup>-1</sup>, respectively [3]. However, today, the concentration of Cr in several rivers and lakes in South America, Europe, and Africa is higher than the threshold value allowed by standards [4]. In Colombia, this contaminant has been detected in the Magdalena River, especially near the mouth of the Bogotá River [5]. In addition, various studies indicate that the levels recorded at monitoring points along the Bogotá River exceed concentrations of 80.4 mg Kg<sup>-1</sup> [6].

\* **CONTACT:** angelica.santisn@campusucc.edu.co

**DOI:** <http://dx.doi.org/10.28991/ESJ-2024-08-01-02>

© 2024 by the authors. Licensee ESJ, Italy. This is an open access article under the terms and conditions of the Creative Commons Attribution (CC-BY) license (<https://creativecommons.org/licenses/by/4.0/>).

Due to health effects, residual effluents containing Cr (VI) ions must be treated before releasing them into the environment or transforming them into less toxic forms [7]. The treatment of this type of effluent is generally carried out by transforming Cr (VI) into Cr (III), which is less harmful and can precipitate in neutral or alkaline conditions to  $\text{Cr}(\text{OH})_3$ , which can be easily disposed of as solid waste [8]. Different methodologies are commonly used to efficiently remove Cr (VI) from aqueous effluents, such as adsorption, electrochemical reduction, microbial reduction, ion exchange, membrane separation, and photocatalytic degradation [9]. The latter, commonly called photocatalysis, is an oxidation process that uses a significant amount of radiation (solar or ultraviolet) and water and does not generate hazardous byproducts. Compared to conventional methods, photocatalysis is environmentally friendly, low-cost, and highly stable [10].

Conventionally, heterogeneous photocatalysis from Cr (VI) to Cr (III) has used  $\text{TiO}_2$ , ZnO, and  $\text{SiO}_2$  [11], widely used photocatalysts, to remove environmental contaminants in the presence of ultraviolet light [12]. Due to its high chemical stability, high durability, low toxicity, hydrophilic nature, high adsorption in the ultraviolet or visible region, and relatively low cost,  $\text{TiO}_2$  is the most widely used photocatalyst, both in suspension and in supported form, in treating Cr (VI) from liquid effluents [13].

Different parameters, such as the initial concentration of the Cr(VI), loading of the photocatalyst, pH of the solution, and particle size of  $\text{TiO}_2$ , among others, are directly related to the photocatalytic treatment of residual effluents in the presence of  $\text{TiO}_2$ . The pH of the solution significantly affects the photocatalytic reduction of Cr(VI) ions. Ghorab et al. [14] studied the influence of the pH of the solution (1.1, 3.0, 5.3, 7.1, and 9.9) on Cr(VI) reduction. According to the authors, the percentage of Cr(VI) reduction is higher at lower pH; the most significant reduction (100%) was noticed when the pH of the solution was 1.1. Castiblanco et al. [15] evaluated the reduction of Cr(VI) at 3.3, 5.0, and 7.7 pH levels. A reduction of 100 percent was observed at 3.3 pH. Sane et al. [16] reported the highest percentage of Cr (VI) reduction, around 79%, at the lowest pH of the solution, about 4; however, in agreement with the other authors, the acidic conditions are favorable for the Cr (VI) reduction. Additionally, Qian et al. [17] noticed that the photocatalytic activity is improved with pH ranges below 4, making it necessary to adjust the pH of the wastewater when the pH is outside of these ranges.

The reaction time is a crucial parameter in the photocatalytic process. Wu et al. [18] found a higher degradation efficiency when experiments were conducted at low rather than high reaction times. This trend agrees with Zhang et al. [19], who reported that removal efficiency was higher at the initial reaction stage. However, the photoreduction efficiency drops markedly with the increase in reaction time.

Likewise, it has been reported that the rate of photocatalysis increases with the mass of the catalyst towards a limit value of high  $\text{TiO}_2$  concentration. This limit depends on the geometry and working conditions of the photoreactor and on a defined amount of  $\text{TiO}_2$  in which the exposed surface is fully illuminated [20]. When the catalyst concentration is very high, turbidity prevents further light penetration into the reactor after traveling a certain distance in an optical path. In any given application, the catalyst mass must be found to avoid excess catalyst and ensure complete and efficient absorption of photons to achieve this optimum [13]. Different articles report the influence of the catalyst concentration on the efficiency of the photocatalytic process. According to Ghorab et al. [14], when the catalyst concentration has increased, the reduction percentage decreases and, after that, remains constant. Sane et al. [16] informed us about increased Cr(VI) reduction when catalyst loading increases.

The results are very different, but from all of them, it can be deduced that the incident radiation in the reactor and the length of the path inside the reactor are essential to determining the optimal concentration of the catalyst [18]. In the case of solar photoreactors, where the path length is several centimeters, the appropriate catalyst concentration is several hundred milligrams per liter. In this case, the highest speed is reached at lower catalyst concentrations as the photoreactor increases in diameter. Ribao et al. [21] suggest that the interactions between the photocatalyst and the polluting agent are a function of the catalyst material's surface area, reflected in its photocatalytic activity.

The results reported by different authors, in general, showed that removing the Cr(VI) through photocatalysis of  $\text{TiO}_2$  depends on variables such as pH, reaction time, and catalyst mass, among others. However, few studies are addressing the effect of the combination, and there are no statistical studies that focus on the interaction of variables such as particle size, catalyst dosage, and reaction time to identify the optimal conditions that lead to the removal of hexavalent chromium in effluents generated by the plastic chrome plating industry.

On the other hand, analyzing and modeling the relationship between various variables through experimental designs allows predicting and optimizing responses for improving processes, products, and systems. The sequential design procedure allows the evaluation of the corresponding statistical model's linear, quadratic, and interactive relationships [22]. This establishes a robust foundation for decision-making regarding resource utilization efficiency, quality enhancement, and regulation compliance. Consequently, it leads to economic, social, and environmental benefits. By resorting to a response surface methodology such as the Box-Behnken Design, where there is an efficient and structured methodology to explore the complex relationships between multiple variables, it is possible to know a specific response

about the variables in the removal of hexavalent chromium in the water treatment of plastic chromium plating industries in Bogotá. In the same way, considering the level of maturity of the operational conditions in the treatment of effluents, this sector is part of that research horizon to work on.

Furthermore, due to the importance of the particle size, the catalyst dose, and the irradiation time on the photocatalytic activity, this issue requires special attention since the country still needs to be sufficiently studied to date. The main objective of this study is to use the response surface methodology to identify the influence of particle size, catalyst dose, and irradiation time on the photoreduction of Cr (VI) to Cr (III) in wastewater from the plastic chromium plating industries through a Box-Behnken experimental design. The most appropriate conditions for each of the variables are also determined.

In order to provide a comprehensive view of the article, we begin with a contextual framework that clarifies the situation that will be examined throughout the study. Subsequently, the fundamental aspects of the experimental design are detailed, providing a detailed description of the variables that compose it. Once this stage is completed, the article presents the results obtained from the experimental design, delving into an analysis of the impact of particle size, catalyst dosage, and irradiation time in the photocatalysis of hexavalent chromium in wastewater. In the pursuit of identifying the optimal conditions for the variables and ascertaining the highest removal efficiency of Cr(VI), a Box Behnken design was implemented. This involved the derivation of a response surface and the generation of contour graphs, facilitating a lucid visualization of the influence exerted by these variables on the catalytic activity of the system, specifically in terms of Cr(VI) removal.

It is imperative to underscore that the outcomes of the experimental design undergo meticulous scrutiny through an ANOVA analysis. This analytical approach ensures that fundamental assumptions of normality, constant variance, and independence in the error term are met. As a concluding step, the article navigates towards optimizing the obtained design, culminating in presenting the most conducive conditions for efficaciously eliminating the contaminants from the effluents of the industrial context.

## 2- Material and Methods

### 2-1- Samples Collection

The experimental methodology of this study was developed in the city of Bogotá (Colombia). The water samples came from the plastic chromium plating industries, which are characterized by presenting considerable amounts of hexavalent chromium Cr (VI). The collection of the samples was carried out as described in the ASTM D1687-17 standard. The residual water presented a pH of  $9.1 \pm 0.16$  and a Cr (VI) concentration of  $0.96 \text{ mg L}^{-1}$ .

### 2-2- Catalyst Pretreatment

TiO<sub>2</sub> (Sigma Aldrich) as a photocatalyst. The TiO<sub>2</sub> was ground in a Restech PM planetary mill for 20 minutes at 500 rpm. The samples obtained were sieved for 10 minutes in a ROTAP Tyler RX-29-16. The material retained in the 80, 100, and 200 mesh sieves was used for the photocatalytic tests, corresponding to the nominal sizes (0.177, 0.149, and 0.074 mm).

### 2-3- Photocatalytic Test

The photocatalytic activity was carried out in 250-mL Erlenmeyer flasks. The pH of the samples was adjusted to a value of 3.3 using HCl (1N), considering what was reported by Castiblanco et al. [15] Doses of 1.0, 2.0, and 3.0 g L<sup>-1</sup>, times of 15, 30, and 45 minutes, and particle sizes of 0.177, 0.149, and 0.074 mm were evaluated. They were irradiated to test the photocatalytic activity of all samples (light source: 24 mW m<sup>-2</sup> ultraviolet lamps). In each Erlenmeyer flask, magnetic stirrers were included within each sample, allowing a homogeneous mixture and simulating the turbulent regime. The experimental setup is presented in Figure 1.



**Figure 1.** Photocatalytic test of experimental setup

After the time determined within the experimentation, 5 ml aliquots of the treated sample were taken, and the elimination of the contaminant was determined. Tests were performed in triplicate, and contaminant removal was quantified using the Hanna Instruments HI3846 Chromium Test Kit. Cr (VI) reacts with diphenylcarbohydrazide to form a purple coloration under acidic buffer conditions, so the amount of coloration that develops is proportional to the concentration of chromium in the wastewater sample.

The removal efficiency (%R) of the contaminant in each test was calculated based on the difference between the initial concentration ( $C_o$ ) and the final concentration ( $C_f$ ) obtained after treatment (Equation 1):

$$\%R = \frac{C_o - C_f}{C_o} \times 100 \quad (1)$$

The contaminated sample was characterized before and after the treatment, where the pH and the percentage of Cr (VI) were defined. The experimental design that represents the work is a Box-Behnken, which has 13 experiments in total and a central point.

Equation 2 represents the second-order mathematical model that fits the Box-Behnken experimental design, considering all linear, quadratic, and linear interaction terms.

$$y = \beta_0 + \sum \beta_i x_i + \sum \beta_{ii} x_i^2 + \sum \beta_{ij} x_i x_j + \epsilon \quad (2)$$

where  $\beta_0$  is the compensation term,  $\beta_i$  is the dependent term or the linear effect of the input factor  $x_i$ ,  $\beta_{ii}$  is the quadratic effect of the input factor  $x_i$ , and  $\beta_{ij}$  is the linear interaction effect between the input factor  $x_i$  and  $x_j$  [23].

The analysis of the experimental design was carried out with the statistical software Minitab. The design is shown in Table 1.

**Table 1. Experimental Design**

No.	Particle size (mm)	TiO <sub>2</sub> dose (g L <sup>-1</sup> )	Irradiation time (min)
1	0.177	1	30
2	0.074	1	30
3	0.177	3	30
4	0.074	3	30
5	0.177	2	15
6	0.074	2	15
7	0.177	2	45
8	0.074	2	45
9	0.149	1	15
10	0.149	3	15
11	0.149	1	45
12	0.149	3	45
13	0.149	2	30
14	0.149	2	30
15	0.149	2	30

The following chart is presented in Figure 2 to clarify the methodology further.

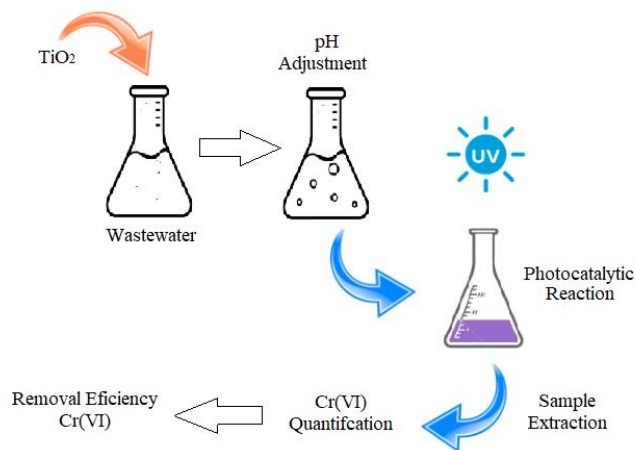


**Figure 2. Methodology**

### 3- Results and Discussion

#### 3-1-Analysis of the Box-Behnken Experimental Design

Factorial fit information for the experimental work is obtained using Minitab software. This information is presented in Table 2.

**Table 2. Factorial adjustment**

Term	Coefficient	SE of coef.	T-value	P-value	IVF
Constant	-0.00	9.04	-0.00	1.000	
Particle size (P)	-3.75	5.53	-0.68	0.528	1.00
Dose (D)	22.50	5.53	4.07	0.010	1.00
Time (T)	6.25	5.53	1.13	0.310	1.00
P*P	15.00	8.15	1.84	0.125	1.01
D*D	27.50	8.15	3.38	0.020	1.01
T*T	-15.00	8.15	-1.84	0.125	1.01
P*D	-17.50	7.83	-2.24	0.076	1.00
P*T	0.00	7.83	0.00	1.000	1.00
D*T	12.50	7.83	1.60	0.171	1.00

Based on the information obtained previously, the regression equation obtained for the design work in this work is presented in Equation 3.

$$\%Remotion = -3,75 P + 22,50 D + 6,25 T + 15,00 P^2 + 27, D^2 - 15T^2 - 17,50PD + 12,50 DT \quad (3)$$

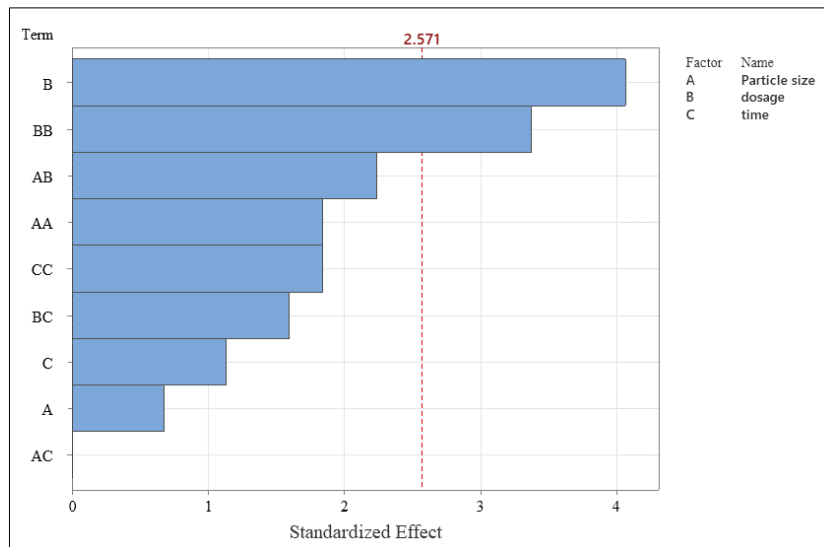
Table 3 presents the analysis of variance of the experimental results.

**Table 3. Analysis of variance**

Source	GL	SC Adj.	MC Adj.	F Value	P Value
Model	9	10948.3	1216.48	4.97	0.046
Linear	3	4475.0	1491.67	6.09	0.040
Particle size (P)	1	112.5	112.50	0.46	0.528
Dose (D)	1	4050.0	4050.00	16.53	0.010
Time(T)	1	312.5	312.50	1.28	0.310
Square	3	4623.3	1541.11	6.29	0.038
P*P	1	830.8	830.77	3.39	0.125
D*D	1	2792.3	2792.31	11.40	0.020
T*T	1	830.8	830.77	3.39	0.125
2-way interactions	3	1850.0	616.67	2.52	0.172
P*D.	1	1225.0	1225.00	5.00	0.076
P*T	1	0.0	0.00	0.00	1.000
D*T	1	625.0	625.00	2.55	0.171
Error	5	1225.0	245.00		
Lack of fit	3	1225.0	408.33	*	*
Pure Error	2	0.0	0.00		
<b>Total</b>	<b>14</b>	<b>12173.3</b>			

The response to the efficiency in removing the pollutant corresponds with a good square fit since the model presents an  $R^2 = 89.94\%$ . Likewise, considering the values of F and p obtained in the analysis, given that F is large and  $p < 0.05$ , the dose factor significantly affects contaminant removal efficiency. In contrast, the primary factors—particle size and time—and their interactions are insignificant since the p values are more significant than 0.05.

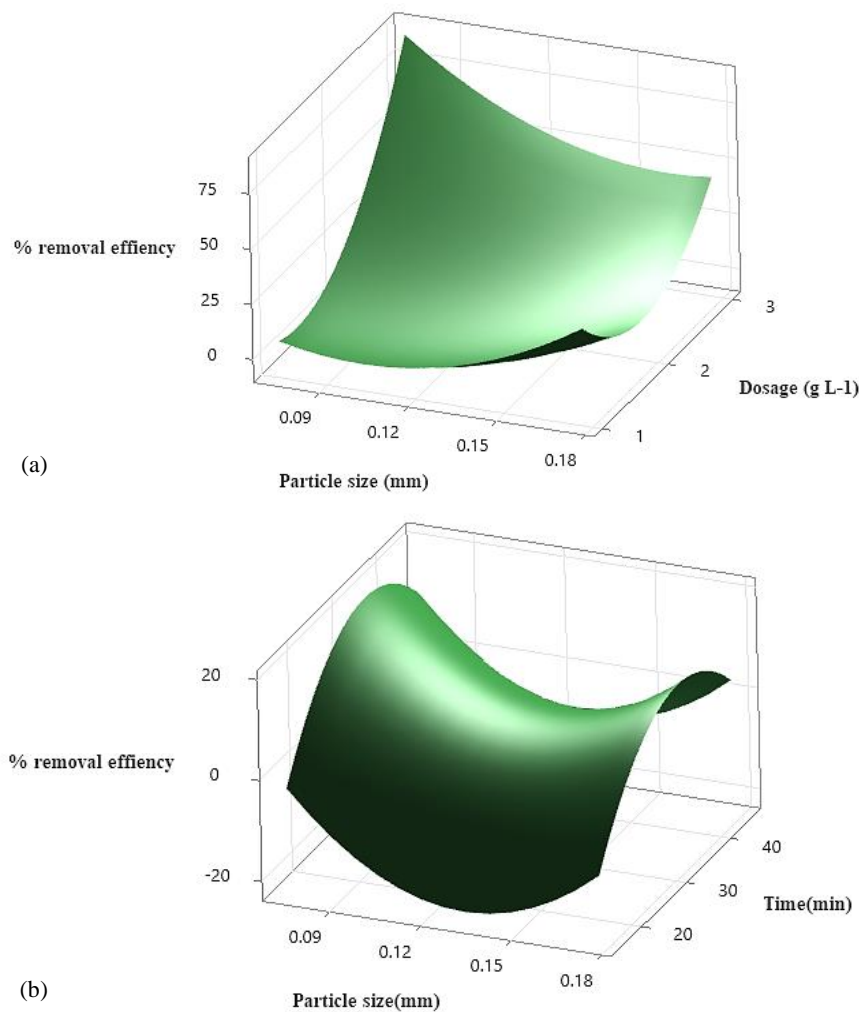
As a complement to what was mentioned above, Figure 3 presents the Pareto chart of the standardized effects that represent a valuable tool in evaluating the relative contribution of the different factors in the model. For its interpretation, it is relevant to note that the values that exceed the vertical reference line are considered significant, indicating their contribution to the model variable. In this context, the bars associated with the dose factor exceed the critical value marked by the red reference line, which denotes potentially statistically significant factors at a confidence level of 0.05. This indicates that increases in the magnitude of the dose factor are statistically associated with a positive effect on pollutant removal. This finding is relevant since it explains the relationship between the applied dose and the efficiency in removing the Cr(VI) under study.



**Figure 3. Pareto Chart of the Standardized Effects**

It is crucial to highlight that, in contrast, neither the interactions nor the other two factors present statistically significant effects on pollutant removal, as evidenced by the p-values greater than 0.05. This information is crucial since it indicates that, among the factors analyzed, the dose is the primary driver of the observed variation in pollutant removal. On the other hand, the categories that do not cross the reference line, including the interactions and the other two factors, exhibit comparatively less influence on the model. This analysis strengthens the coherence and robustness of the results obtained, thus supporting the reliability of the conclusions drawn from the study. Identifying significant factors provides a firm basis for decision-making and suggests specific focus areas for future research or interventions.

The response surfaces of the experiment are observed in Figure 4.



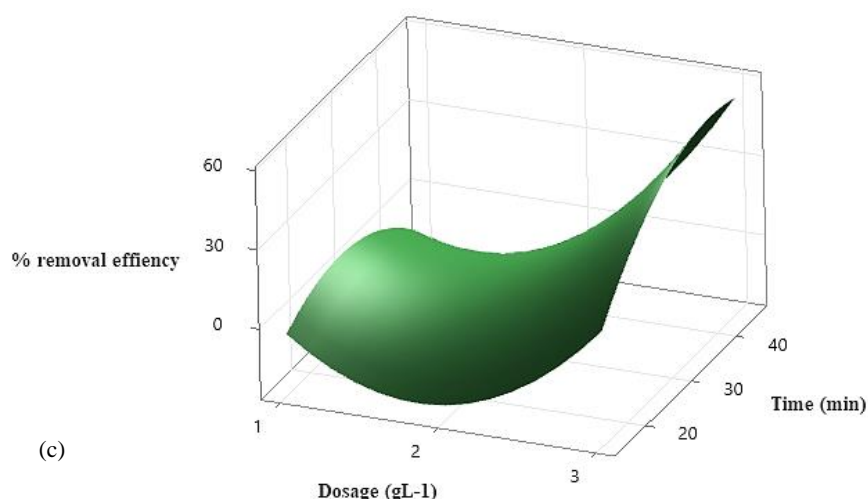


**Figure 4.** Response surfaces for the experimental design obtained a) removal efficiency vs. particle size vs. dose, b) removal efficiency versus particle size versus time, c) removal efficiency vs. dose vs. time

Figures 4-a and 4-b visualize the relationship between the removal percentage and the variables particle size, catalyst dose, particle size, and time, respectively. The crucial influence of particle size on pollutant removal is highlighted (value less than 0.09mm), supporting previous findings reported by various authors. This can be explained by the fact that smaller particles display a larger surface area, promoting the swift diffusion of reagents, a more efficient interfacial reaction, and enhanced light absorption, resulting in a more effective photodegradation process. This phenomenon is attributed to the surface-volume ratio, electron/hole recombination, and active sites on the surface [24, 25]. Although smaller particles offer a shorter diffusion pathway and potentially improve the reaction rate, it is crucial to consider that the specific effects of particle size may vary depending on the application and experimental conditions.

Figure 4-c represents the impact of the catalyst dose (value of 3 gL<sup>-1</sup>), showing a proportional increase in the percentage of chromium removal with increasing photocatalyst dose. At higher loads, removal is more efficient, resulting in a higher removal per unit weight of photocatalyst. Although conditions were found for the rapid elimination of hexavalent chromium, it is essential to note that this requires a relatively high dose [26–29]. However, it is essential to highlight that an excess catalyst can increase turbidity, reduce visible light radiation, and decrease photodegradation efficiency. The top particles of the catalyst tend to aggregate, decreasing the surface area and affecting photon absorption. This results in a decreased reaction rate constant and interference with the mass transfer limitations. Turbidity, induced by an excess of photocatalyst, reduces light transmittance, affecting the intensity of light that reaches the catalyst's surface [25].

Considering Figures 4b and 4c, it is highlighted that the most significant removal is observed when the time is high (approximately 40 min). However, as indicated by Joshi & Shrivastava [29], the combination of the increase in the dose of photocatalysts and the contact time favors the reaction, thus promoting the reduction. In other words, a long contact time drives a higher reduction rate, allowing for prolonged interaction of the reagents and facilitating the reduction process. This prolonged contact can translate into higher efficiency and a stronger interfacial reaction. Furthermore, an extended contact time improves the mass transfer of Cr(VI) to the TiO<sub>2</sub> surface, increasing the reduction rate [25, 30, 31]. Although a longer contact time promotes effective reduction, determining the optimal contact time will depend on several factors, and further research is required to determine its specific effect on Cr (VI) removal by photocatalysis.

To support the information obtained in Figure 4, contour charts have been used as an additional resource to provide a more accurate representation. This analysis presents the contours derived from the experimental design, detailed in Figure 5. These contour charts provide a more detailed visualization of the relationships between the evaluated variables, highlighting the areas of maximum efficiency in pollutant removal. This approach is an effective way of identifying ideal conditions, as it provides a more transparent and understandable visual representation. The graphical presentation of the contours facilitates interpretation by vividly highlighting areas where the pollutant removal efficiency peaks. This refinement in data presentation contributes significantly to a more robust and accurate interpretation of the experimental design results, improving the clarity and general understanding of the relationship between the variables studied.

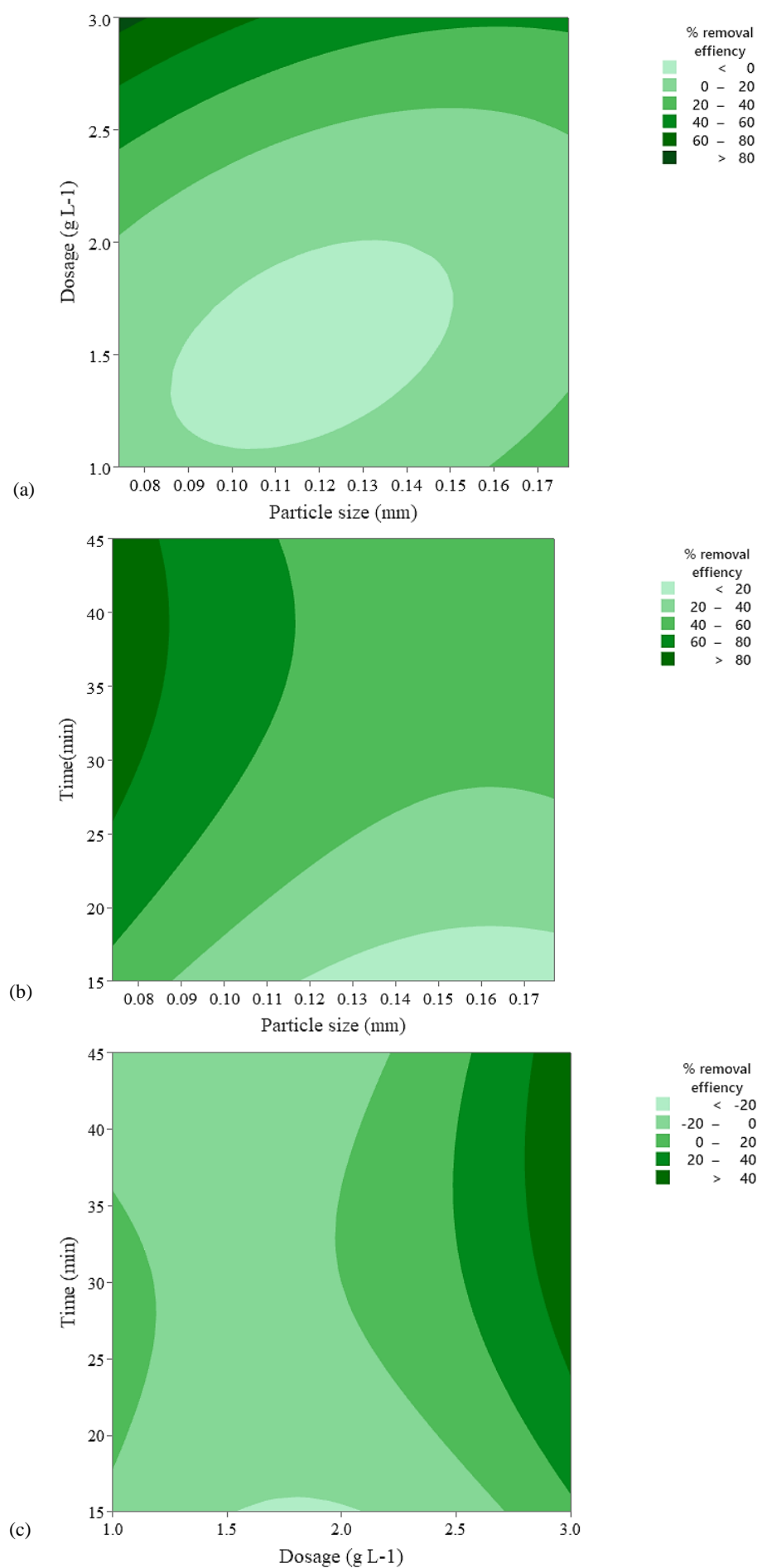


**Figure 5.** Contour plots for removing hexavalent chromium: a) particle size vs dose; b) particle size vs. time; c) dose vs time

As evidenced in Figures 5-a, 5-b, and 5-c, the contour charts are presented, where a color gradient is highlighted that indicates removal levels, with darker shades of green representing higher values, while lighter shades indicate low values. In Figures 5a and 5b, the darker bands, which indicate a pollutant removal more significant than 80%, are located in the range where the dose is approximately  $3 \text{ gL}^{-1}$ , the particle size is less than 0.08 mm, and the time is close to 40 min, and the particle size is less than 0.08mm, respectively.

On the other hand, in Figure 5c, the contour chart reveals that removal more significant than 40% occurs in a range where times are greater than 35 minutes and the catalyst dose is approximately  $3 \text{ gL}^{-1}$ . Considering these results and the information from all the contour graphs made with the experimental values, it is concluded that the optimal removal conditions are reached when the particle size is less than 0.08 mm, the dose is  $3 \text{ gL}^{-1}$ , and the time is approximately 40 minutes.

Based on the previous data and the results obtained, an optimization was carried out to determine a more accurate estimate of the optimal conditions for the most significant removal of hexavalent chromium. Given the need for precision and reliability in configuring these variables, the optimization was carried out efficiently, maximizing both time and resources. The results of this optimization are detailed in Table 4.

**Table 4. Optimization of the response (% removal efficiency)**

<b>Parameters</b>						
<b>Response</b>	<b>Goal</b>	<b>Lower</b>	<b>Target</b>	<b>Upper</b>	<b>Weight</b>	<b>Importance</b>
% removal efficiency	Maximum	0	100		1	1
<b>Solution</b>	<b>Particle size</b>	<b>Dosage</b>	<b>Time</b>	<b>%Removal efficiency fit</b>	<b>Composite Desirability</b>	
1	0.074	3	39.2424	92.1082	0.921082	1
<b>Multiple Response Prediction</b>						
<b>Variable</b>	<b>Setting value</b>					
Particle size	0.074					
Dose	3					
Time	39.2424					
<b>Response</b>	<b>Fit</b>	<b>SE Fit</b>	<b>95% CI</b>	<b>95% PI</b>		
% removal efficiency	92.1	15.1	(53.3; 130.9)	(36.2; 148.0)		

Considering the information in Table 4, the optimal values for removing the contaminant correspond to a particle size of 0.074 mm, a dose of  $3 \text{ gL}^{-1}$ , and a time of 39.2424 min.

#### 4- Conclusions

This study was proposed to address the problem of hexavalent chromium contamination in wastewater from plastic chromium plating industries, focusing on optimizing the photocatalysis process. The process was implemented through a Box-Behnken experimental design, where the conditions of particle size, catalyst dose, and irradiation time were varied to determine their impact on the photoreduction efficiency of Cr(VI) to Cr(IV).

The results revealed that the particle size of 0.074 mm exhibited the highest photocatalytic activity, achieving 100% removal of the contaminant in just 45 minutes of irradiation, compared to particle sizes of 0.149 mm and 0.074 mm. Furthermore, thanks to the experimental design, an equation was derived that allowed the process to be adjusted, and the optimal conditions for each of the variables were identified, where it was obtained for the particle size and dose (0.074 mm and  $3 \text{ gL}^{-1}$ ), along with a time of 39.2424 min. These results represent a significant advance in mitigating pollution in the plastic chromium plating industries, directly contributing to the preservation of water resources. In addition, identifying optimal conditions for the variables studied provides valuable guidance for future applications and improvements in wastewater treatment processes in this sector.

It is essential to highlight that the response surface methodology (Box-Behnken Design) provides valuable insights into the specific problem covered in this article. Likewise, this methodology could lay the foundations for future research treating industrial effluents.

In summary, this study has contributed to the scientific knowledge of hexavalent chromium removal and provides valuable insights for the practical application of photocatalysis in industrial wastewater decontamination.

## 5- Declarations

### 5-1-Author Contributions

Conceptualization, A.S. and O.A.; methodology, A.S. and O.A.; validation, L.A.C., J.C., and P.V.; formal analysis, A.S., O.A, P.V., L.A.C., and J.C.; data curation, L.A.C., J.C., and P.V.; writing—original draft preparation, L.A.C., J.C., and A.S.; writing—review and editing, A.S. and O.A.; project administration, A.S. All authors have read and agreed to the published version of the manuscript.

### 5-2-Data Availability Statement

The data presented in this study are available on request from the corresponding author.

### 5-3-Funding

The authors thank the Universidad Cooperativa for the INV3095 project.

### 5-4-Institutional Review Board Statement

Not applicable.

### 5-5-Informed Consent Statement

Not applicable.

### 5-6-Conflicts of Interest

The authors declare that there is no conflict of interest regarding the publication of this manuscript. In addition, the ethical issues, including plagiarism, informed consent, misconduct, data fabrication and/or falsification, double publication and/or submission, and redundancies have been completely observed by the authors.

## 6- References

- [1] Acharya, R., Naik, B., & Parida, K. (2018). Cr(VI) remediation from aqueous environment through modified-TiO<sub>2</sub>-mediated photocatalytic reduction. *Beilstein Journal of Nanotechnology*, 9(1), 1448–1470. doi:10.3762/bjnano.9.137.
- [2] Karimi-Maleh, H., Ayati, A., Ghanbari, S., Orooji, Y., Tanhaei, B., Karimi, F., Alizadeh, M., Rouhi, J., Fu, L., & Sillanpää, M. (2021). Recent advances in removal techniques of Cr(VI) toxic ion from aqueous solution: A comprehensive review. *Journal of Molecular Liquids*, 329, 115062. doi:10.1016/j.molliq.2020.115062.
- [3] Azeez, N. A., Dash, S. S., Gummadi, S. N., & Deepa, V. S. (2021). Nano-remediation of toxic heavy metal contamination: Hexavalent chromium [Cr(VI)]. *Chemosphere*, 266, 129204. doi:10.1016/j.chemosphere.2020.129204.
- [4] Aigbe, U. O., & Osibote, O. A. (2020). A review of hexavalent chromium removal from aqueous solutions by sorption technique using nanomaterials. *Journal of Environmental Chemical Engineering*, 8(6), 104503. doi:10.1016/j.jece.2020.104503.
- [5] IDEAM. (2023). National Water Study 2022. Institute of Hydrology, Meteorology and Environmental Studies (IDEAM), Bogota, Colombia.
- [6] Avila Triviño, J. J., & Larrota Paz, I. (2021). Analysis of concentrations of mercury, hexavalent chromium in water from the Magdalena River, as a source of supply for human consumption in Girardot-Ricaurte. Universidad Piloto de Colombia, Bogota, Colombia.
- [7] Wu, Z., Chen, R., Gan, Q., Li, J., Zhang, T., & Ye, M. (2018). Mesoporous Na<sup>+</sup>-SiO<sub>2</sub> spheres for efficient removal of Cr<sup>3+</sup> from aqueous solution. *Journal of Environmental Chemical Engineering*, 6(2), 1774–1782. doi:10.1016/j.jece.2018.02.025.
- [8] Tahir, M. B., Kiran, H., & Iqbal, T. (2019). The detoxification of heavy metals from aqueous environment using nano-photocatalysis approach: a review. *Environmental Science and Pollution Research*, 26(11), 10515–10528. doi:10.1007/s11356-019-04547-x.
- [9] Islam, M. M., Mohana, A. A., Rahman, M. A., Rahman, M., Naidu, R., & Rahman, M. M. (2023). A Comprehensive Review of the Current Progress of Chromium Removal Methods from Aqueous Solution. *Toxics*, 11(3), 252. doi:10.3390/toxics11030252.
- [10] Yuan, G., Li, F., Li, K., Liu, J., Li, J., Zhang, S., Jia, Q., & Zhang, H. (2021). Research progress on photocatalytic reduction of Cr(VI) in polluted water. *Bulletin of the Chemical Society of Japan*, 94(4), 1142–1155. doi:10.1246/bcsj.20200317.
- [11] Lathe, A., & Palve, A. M. (2023). A review: Engineered nanomaterials for photoreduction of Cr(VI) to Cr(III). *Journal of Hazardous Materials Advances*, 12, 100333. doi:10.1016/j.hazadv.2023.100333.
- [12] Naik, B., Nanda, B., Das, K. K., & Parida, K. (2017). Enhanced photocatalytic activity of nanoporous BiVO<sub>4</sub>/MCM-41 co-joined nanocomposites for solar energy conversion and environmental pollution abatement. *Journal of Environmental Chemical Engineering*, 5(5), 4524–4530. doi:10.1016/j.jece.2017.08.045.

- [13] Katal, R., Masudy-Panah, S., Tanhaei, M., Farahani, M. H. D. A., & Jiangyong, H. (2020). A review on the synthesis of the various types of anatase TiO<sub>2</sub> facets and their applications for photocatalysis. *Chemical Engineering Journal*, 384. doi:10.1016/j.cej.2019.123384.
- [14] Ghorab, M. F., Djellabi, R., & Messadi, R. (2013). Photo-reduction of Hexavalent Chromium in Aqueous Solution in the Presence of TiO<sub>2</sub> as Semiconductor Catalyst. *E3S Web of Conferences*, 1, 25008. doi:10.1051/e3sconf/20130125008.
- [15] Castiblanco, Y., Perilla, A., Arbelaez, O., Velásquez, P., & Santis, A. (2021). Effect of the pH and the catalyst concentration on the removal of hexavalent chromium (Cr (VI)) during photocatalysis of wastewater from plating on plastics industry. *Chemical Engineering Transactions*, 86, 679–684. doi:10.3303/CET2186114.
- [16] Sane, P., Chaudhari, S., Nemade, P., & Sontakke, S. (2018). Photocatalytic reduction of chromium (VI) using combustion synthesized TiO<sub>2</sub>. *Journal of Environmental Chemical Engineering*, 6(1), 68–73. doi:10.1016/j.jece.2017.11.060.
- [17] Qian, R., Zong, H., Schneider, J., Zhou, G., Zhao, T., Li, Y., Yang, J., Bahnemann, D. W., & Pan, J. H. (2019). Charge carrier trapping, recombination and transfer during TiO<sub>2</sub> photocatalysis: An overview. *Catalysis Today*, 335, 78–90. doi:10.1016/j.cattod.2018.10.053.
- [18] Wu, Q., Zhao, J., Qin, G., Wang, C., Tong, X., & Xue, S. (2013). Photocatalytic reduction of Cr(VI) with TiO<sub>2</sub> film under visible light. *Applied Catalysis B: Environmental*, 142–143, 142–148. doi:10.1016/j.apcatb.2013.04.056.
- [19] Zhang, X., Song, L., Zeng, X., & Li, M. (2012). Effects of Electron Donors on the TiO<sub>2</sub> Photocatalytic Reduction of Heavy Metal Ions under Visible Light. *Energy Procedia*, 17, 422–428. doi:10.1016/j.egypro.2012.02.115.
- [20] Marinho, B. A., Djellabi, R., Cristóvão, R. O., Loureiro, J. M., Boaventura, R. A. R., Dias, M. M., Lopes, J. C. B., & Vilar, V. J. P. (2017). Intensification of heterogeneous TiO<sub>2</sub> photocatalysis using an innovative micro-meso-structured-reactor for Cr(VI) reduction under simulated solar light. *Chemical Engineering Journal*, 318, 76–88. doi:10.1016/j.cej.2016.05.077.
- [21] Ribao, P., Corredor, J., Rivero, M. J., & Ortiz, I. (2019). Role of reactive oxygen species on the activity of noble metal-doped TiO<sub>2</sub> photocatalysts. *Journal of Hazardous Materials*, 372, 45–51. doi:10.1016/j.jhazmat.2018.05.026.
- [22] Li, Z., Lu, D., & Gao, X. (2021). Optimization of mixture proportions by statistical experimental design using response surface method - A review. *Journal of Building Engineering*, 36, 102101. doi:10.1016/j.jobe.2020.102101.
- [23] Giri, A. K., & Mishra, P. C. (2023). Optimization of different process parameters for the removal efficiency of fluoride from aqueous medium by a novel bio-composite using Box-Behnken design. *Journal of Environmental Chemical Engineering*, 11(1), 82283877. doi:10.1016/j.jece.2022.109232.
- [24] Rashid, M. M., Simončič, B., & Tomšič, B. (2021). Recent advances in TiO<sub>2</sub>-functionalized textile surfaces. *Surfaces and Interfaces*, 22, 100890. doi:10.1016/j.surf.2020.100890.
- [25] Suhan, M. B. K., Al-Mamun, M. R., Farzana, N., Aishee, S. M., Islam, M. S., Marwani, H. M., Hasan, M. M., Asiri, A. M., Rahman, M. M., Islam, A., & Awual, M. R. (2023). Sustainable pollutant removal and wastewater remediation using TiO<sub>2</sub>-based nanocomposites: A critical review. *Nano-Structures and Nano-Objects*, 36. doi:10.1016/j.nanoso.2023.101050.
- [26] Pechishcheva, N. V., Ordinartsev, D. P., Valeeva, A. A., Zaitceva, P. V., Korobitsyna, A. D., Sushnikova, A. A., Petrova, S. A., Shunyaev, K. Y., & Rempel, A. A. (2023). Photoadsorption of Cr(VI) on titanium dioxide modified by high-energy milling. *Inorganic Chemistry Communications*, 154, 110968. doi:10.1016/j.inoche.2023.110968.
- [27] Kandasamy, S., Velusamy, S., Thirumoorthy, P., Periyasamy, M., SenthilkumarVeerasamy, Gopalakrishnan, K. M., ... & Periyasamy, S. (2022). Adsorption of chromium ions from aqueous solutions by synthesized nanoparticles. *Journal of Nanomaterials*, 2022, 1-8. doi:10.1155/2022/6214438.
- [28] Stancl, H. O. N., Hristovski, K., & Westerhoff, P. (2015). Hexavalent Chromium Removal Using UV-TiO<sub>2</sub>/Ceramic Membrane Reactor. *Environmental Engineering Science*, 32(8), 676–683. doi:10.1089/ees.2014.0507.
- [29] Joshi, K. M., & Shrivastava, V. S. (2011). Photocatalytic degradation of Chromium (VI) from wastewater using nanomaterials like TiO<sub>2</sub>, ZnO, and CdS. *Applied Nanoscience (Switzerland)*, 1(3), 147–155. doi:10.1007/s13204-011-0023-2.
- [30] Djellabi, R., Su, P., Elimian, E. A., Poliukhova, V., Nouacer, S., Abdelhafeez, I. A., Abderrahim, N., Aboagye, D., Andhalkar, V. V., Nabgan, W., Rtimi, S., & Contreras, S. (2022). Advances in photocatalytic reduction of hexavalent chromium: From fundamental concepts to materials design and technology challenges. *Journal of Water Process Engineering*, 50. doi:10.1016/j.jwpe.2022.103301.
- [31] Yang, C. C., Dao, K. C., Lin, Y. S., Cheng, T. Y., Chen, K. F., & Tsai, Y. P. (2021). Impacts of mixing mode on photocatalytic reduction of hexavalent chromium over titanium dioxide nanomaterial under various environmental conditions. *Water (Switzerland)*, 13(16), 2291. doi:10.3390/w13162291.